Journal Pre-proof

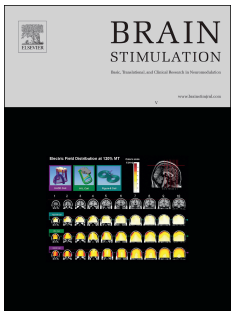

BurstDR spinal cord stimulation rebalances pain input and pain suppression in the brain in chronic neuropathic pain

Sven Vanneste, Dirk De Ridder

PII: S1935-861X(23)01872-7

DOI: https://doi.org/10.1016/j.brs.2023.07.058

Reference: BRS 2434

To appear in: *Brain Stimulation*

Received Date: 26 January 2023

Revised Date: 6 July 2023

Accepted Date: 31 July 2023

Please cite this article as: Vanneste S, De Ridder D, BurstDR spinal cord stimulation rebalances pain input and pain suppression in the brain in chronic neuropathic pain, *Brain Stimulation* (2023), doi: https://doi.org/10.1016/j.brs.2023.07.058.

BurstDR spinal cord stimulation rebalances pain input and pain suppression in the brain in chronic neuropathic pain.

Sven Vanneste[1] & Dirk De Ridder[2]

1. Global Brain Health Institute, Institute of Neuroscience, Trinity College Dublin, Dublin, Ireland.
2. Department of Surgical Sciences, Section of Neurosurgery, Dunedin School of Medicine, University of Otago, New Zealand.

Short title: Pain as a brain imbalance problem

Keyword: Chronic pain, burst, spinal cord stimulation, medial suffering pathway, lateral painfulness pathway, descending pain inhibitory pathway

Correspondence: Sven Vanneste, Lab for Clinical & Integrative Neuroscience, Global Brain Health Institute and Institute of Neuroscience, Trinity College Dublin, College Green, Dublin 2, Ireland. email: sven.vanneste@tcd.ie; website: http://www.lab-clint.org

Abstract

Objective: Chronic pain is processed by at least three well-known pathways, two pain provoking pathways including a medial 'suffering' and lateral 'painfulness' pathway. A third descending pain pathway modulates pain but is predominantly inhibitory. Chronic pain can be seen as an imbalance between the two pain-provoking and the pain inhibitory pathways. If this assumption is correct, then the imbalance between pain input and pain suppression should reverse and *normalize* in response to successful, i.e., pain reducing burstDR spinal cord stimulation, one of the current treatment options for neuropathic pain.

Materials and Methods: Fifteen patients, who received spinal cord stimulation for failed back surgery were included in this study, using source localized electrical brain activity and connectivity recording via EEG to identify the purported imbalance.

Results: BurstDR spinal cord stimulation induces a significant change in EEG activity in both the left and right somatosensory cortex (SSC) for both θ and γ oscillations. In the dorsal anterior cingulate cortex (dACC), we observed a significant drop in both α and β oscillations. This reduction is accompanied by a change in pain intensity and suffering. BurstDR spinal cord stimulation is also associated with a reduction in θ at the pregenual anterior cingulate cortex (pgACC). Analyzing effective connectivity indicates that for the θ band, more information is sent from the pgACC to the left and right SSC. For α, increased information is sent from the pgACC to the dACC and both the left and right SSC. This is associated with a reduced θ-γ coupling in the SSC and reduced α-β coupling in dACC.

Conclusion: This study suggests that chronic pain is indeed an imbalance between the ascending and descending pathways in the brain and that burst spinal cord stimulation can normalize this imbalance in the brain.

Introduction

Over one-third of the world's population suffers from persistent or chronic pain, resulting in tremendous burden for the individual[1] and society[2]. The subjective experience of chronic pain results from pathological brain network interactions, rather than from persisting physiological sensory input via nociceptors[1]. Pain is processed by three well-known pathways[3-8]. The two ascending pathways include the anatomically and functionally separable medial and lateral pain pathway[3, 9-11]. The medial pain pathway, which involves the dorsal anterior cingulate cortex (dACC) and anterior insula as main hubs, encodes the unpleasantness and suffering of pain[3, 4, 9-11]. The lateral pathway, which involves the somatosensory cortex (SSC) as major hub, processes the discriminatory/sensory components of the pain[9-12]. In addition, a descending pain inhibitory pathway[6] involves the rostral and pregenual anterior cingulate cortex (pgACC), hypothalamus, and periaquaductal gray (PAG). The PAG connects to serotoninergic nucleus raphe magnus (NRM) as well as to thenucleus reticularis gigantocellularis-pars alpha and the nucleus paragigantocellularis lateralis of the rostral ventromedial medulla oblongata. These two nuclei connect to the noradrenergic nucleus reticularis lateralis (NRL). Both the serotoninergic NRM and noradrenergic NRL project to the dorsal horn of the spinal cord, modulating somatosensory input[5-7, 10, 11, 13, 14]. This descending pathway is responsible for stress-mediated pain inhibition[15], and placebo analgesia[7, 13].

Recent research has theorized chronic pain as an imbalance between brain areas involved in ascending and descending pain pathways[16-18]. This imbalance is controlled by different brain oscillations that all contribute in routing of information flow between brain areas involved in pain input and pain suppression[19]. That is, as proposed by the thalamococrtical dysrhythmia model[20], chronic pain is associated with a reduction in resting state alpha power and increased θ and γ oscillations in the SSC. The increased γ band activity in the SSC correlates

with intensity of chronic pain, similar to what is noted in acute experimental pain[19, 21-23]. The dACC accelerates from θ to α and β frequencies, suggesting an increase in pain suffering. The descending pain inhibitory system with the pgACC as main hub normally oscillates at rest in θ[24]. For chronic pain patients the descending pain inhibitory system accelerates from θ to α suggesting that pain suppression is paradoxically increased, possibly as an attempt, albeit insufficient, to compensate for the increase in pain input[10].

An implicit assumption related to the imbalance model posits that pain can improve either by reducing pain input and/or increasing pan suppression or a combination of both[10]. Spinal cord stimulation is used to treat neuropathic pain, failed back surgery, complex regional pain, angina pectoris, metabolic and ischemic limb pain [25-28]. Research has shown that spinal cord stimulation induces a reduction in somatosensory evoked potentials, suggesting that spinal cord stimulation inhibits cortical somatosensory processing [29, 30]. Furthermore, a review of the effects of spinal cord stimulation on spectral features in resting-state electroencephalography identified revealed changes in activity in the studied frequency bands, i.e. theta [4-7.5 Hz], alpha [8-12.5 Hz], beta [13-30 Hz], and gamma [30+ Hz]) [31]. The eight included EEG studies identified modulation of of the medial, lateral and descending pain pathways for paresthesia-free spinal cord stimulation paradigms, and lateral and descending pain pathways fortraditional tonic stimulation[31]. Indeed, EEG research shows that tonic spinal cord stimulation mainly modulates the lateral and descending pathway, while burstDR spinal cord stimulation modulates the medial descending pathway as well[8, 17]. These findings were further confirmed using Fluorodeoxyglucose Positron Emission Tomography [33].Moreover, multiple of the included studies reported an increased alpha peak frequency, increased alpha power, and/or decreased theta power when SCS was compared with baseline, indicating modulation of thalamocortical pathways[31]. One form of spinal cord stimulation is burstDR spinal cord stimulation, applying small bursts of monophasic pulses charge balanced after the pulses[17,

34, 35]. Functional imaging studies in spinal cord stimulation have shown that a decrease in perceived pain intensity and pain quality correlates with changes in the dACC, SSC as well as pgACC that are part of the medial, lateral, and descending pathway, respectively[8, 10, 17, 34, 36, 37]. If the balance model is correct, the signature of the imbalance between pain input and pain suppression should reverse and *normalize* in response to burstDR stimulation.

A balance, by definition, requires communication between areas that are involved in pain input and suppression such as the dACC, SSC, and pgACC. Thus, the lack of communication, as demonstrated by decreased functional connectivity between pain input and pain suppression, results in a loss of balance between interacting areas[16]. Indeed, functional connectivity changes have been identified between dACC, SSC, and pgACC for both the θ and α band[16]. This communication deficit is associated with increased θ-γ coupling in the SSC[16], which is consistent with the thalamocortical dysrhythmia model of pain that proposes that α-γ nesting is a physiological mechanism transmitting sensory information and that slowed down alpha into the θ range reflects pathological θ-γ coupling, associated with tinnitus and pain[20, 38, 39].

Based on a cross-sectional analysis an imbalance between pain input and pain suppression in the brain pathways, rather than an isolated increase in pain input, was already suggested as the underlying mechanism of chronic pain perception[10, 11, 16]. The goal of this study is to further explore the proposed hypothesis that chronic pain is indeed the result of a persisting quantifiable and thus measurable imbalance between pain input and pain suppression in the brain involving different neuronal oscillations. Based on the thalamocortical dysrhythmia model of chronic pain[20, 40-42] and the imbalance model[10, 11, 16], we expect that suppression of chronic pain is associated with both activity and connectivity changes. For activity we expect a spinal cord stimulation induced increase in α and decrease in θ and γ oscillations in the SSC, as well as changes in the θ, α and β frequencies in the dACC and pgACC. A balance requires communication, i.e. connectivity, between areas that are involved

in pain input and suppression. Consequently, we expect that SCS improves the communication and thus connectivity between dACC, SSC, and pgACC, i.e. shows a tendency to normalization.

Methods and Materials

Participants

Fifteen patients, 9 men and 6 women, were included in this study. Patients' ages range between 40 and 67 years, with a mean of 53.22 years (Sd = 9.34). The 15 consecutive patients presenting at the neuromodulation clinic of the University Hospital Antwerp, Belgium were eligible for spinal cord stimulation according to the Belgian requirements for reimbursement for spinal cord stimulation, which states that the patient has to be medically intractable to opioids and antiepileptic drugs were included. All patients were selected by the neurosurgeon Dirk De Ridder, and after multidisciplinary discussion with a specialized pain physician, a psychological and psychiatric evaluation was performed to rule out psychogenic pain as well as other psychiatric morbidity contraindicating an implant. After authorization by the psychologist and psychiatrist, as mandatory by the Belgian health system, an implant was offered. The study was in accordance with the ethical standards of the Helsinki declaration (1964) and was approved by the institutional ethics committee (UZA OGA85).

Implantation

The data was collected before 2017. All patients underwent a surgical implantation of a Lamitrode 88 (St. Jude Medical neurodivision, Plano, TX, USA) via laminectomy under general anesthesia. An initial programming session was performed for one week in tonic mode to define which electrodes covered the painful body area, as determined by paresthesia coverage. The patients' internal pulse generator (IPG) was programmed while lying down. The patients were discharged on the second postoperative day and were instructed not to change the stimulation

parameters during the next week. They were only allowed to use a magnet for forcefully stopping stimulation in case of emergency. Reprogramming consisted of first turning off the stimulator and when the patient mentioned the pain had recurred to its prestimulation level, the new stimulation set was applied. Both the patient, the physician as outcome assessor as well as the statistician were blinded to exact parameters (e.g., amplitude, electrode configuration), only the programmer was aware of the settings. As the Belgian reimbursement system at the time of the study mandated a minimum of 28 days of externalized stimulation, the 3 weeks of burst stimulation was performed to find the optimal settings using a non-sterile EON® (SJMedical, Plano, TX, USA) IPG via externalized extension wires. After the final implantation of the IPG, patients were programmed using the parameters that resulted in maximal pain suppression. Patients came back six months after the IPG implantation for final assessment.

The burst mode was programmed using a custom-made software and programming device. Typically, burst stimulation is characterized by a lower amplitude, but larger pulse width, resulting in a similar energy delivery per pulse[35]. In burst mode the amplitude was increased up to the moment that paresthesias were elicited. Subsequently the amplitude was decreased to a level below paresthesia threshold.

The cumulative charge of the five 1 ms spikes is balanced during 5 ms following the monophasic spikes, and charge balancing is not performed after each individual spike, as this mimics intermittent tonic firing, rather than true burst firing[43-45]. This differentiates burst mode from intermittent high frequency stimulation[43].

Assessments

Primary outcome measures were the pain Visual Analogue Scale (VAS) consisting of a 100-mm line for general pain. General pain is defined as a global pain score experienced during the past week, not specifying axial or limb pain. The secondary outcome measure was pain

catastrophizing scale (PCS). The PCS indicates the catastrophizing impact of pain experienced by the patient. It consists of 13 statements concerning pain experiences on a 5-point scale[46]. Both outcome measures were collected via written assessments before implantation and after the third week of burstDR stimulation where all settings were stable for at least one week.

Electroencephalogram (EEG)

1. Recordings

Electroencephalography (EEG) data (Neuroscan, http://compumedicsneuroscan.com/) were obtained in a quiet room while each participant was sitting upright on a comfortable chair. The scalp was cleaned with alcohol wipes before the baseline EEG recording. The EEG was sampled with 19 electrodes in the standard 10–20 International placement and impedances were checked to remain below 5 kΩ. Data were collected eyes-closed (sampling rate = 1 kHz, band passed DC–200 Hz) and lasted approximately 5 min. The midline reference was located at the vertex and the ground electrode was located at AFZ. Participants were instructed not to drink alcohol 24 hours prior to EEG recording or caffeinated beverages one hour before recording to avoid alcohol- or caffeine-induced changes in the EEG stream [47-49]. The alertness of participants was checked by monitoring both slowing of the alpha rhythm and appearance of spindles in the EEG stream to prevent possible enhancement of the theta power due to drowsiness during recording[50]. The EEGs are performed before and the end of at least week of burst stimulation. While recording the EEG, the IPG was switched-off to avoid artefacts in the EEG. The IPG was switched-off immediately before EEG recording, while pain reduction was maintained due to residual inhibition for a longer time than the EEG recording. Off-line data were resampled to 128 Hz, band-pass filtered in the range 2–44 Hz and subsequently transposed into Eureka! software[51], plotted and carefully inspected for manual artifact-

rejection. All episodic artifacts including eye blinks, eye movements, teeth clenching, body movement, or ECG artifacts were removed from the stream of the EEG.

A careful inspection of artifacts was performed and all episodic artifacts suggestive of eye blinks, eye movements, jaw tension, teeth clenching, or body movement were manually removed from the EEG stream. An artifact was defined as an EEG characteristic that differs from signals generated by activity in the brain [42]. 1) Some artifacts are known to be in a limited frequency range, e.g., above some frequency. These were removed by frequency filtering. 2) Some artifacts consist of discrete frequencies such as 50 Hz or its harmonics. These were removed by notch filtering. 3) Some artifacts are limited to a certain time range, e.g., in the case of eye blinks. These artifacts were recognized by visual inspection and these time intervals were discarded. 4) Some artifacts originate from one or a few distinct sources or a limited volume of space so that the artifact topography is a superposition of characteristic topographies (equivalently, the artifact is limited to a subspace of the signal space). We removed these artifacts by determining the characteristic topographies (equivalently, the artifact subspace) so that the remaining signals do not contain anything from the artifact subspace. 5) Artifacts and true brain signals that can be assumed to be sufficiently independent can be removed by independent component analysis. 6) Some artifacts are characterized by a temporal pattern such as exponential decay. We removed these artifacts by modeling the artifact and fitting its parameters to the data and then removing the artifact. The average length of the EEG after artefact rejection was 4.23 minutes with a minimum of 3.91 minutes.

2. Region of interest analysis

Exact low-resolution brain electromagnetic tomography (eLORETA, available at https://www.uzh.ch/keyinst/) is a functional imaging method yielding standardized current density with zero localization error based on certain electrophysiological and neuroanatomical

constraints[52]. eLORETA was utilized to estimate the intracerebral sources generating the scalp-recorded electrical activity in each of the following five frequency bands: θ (4–7.5 Hz), α (8–12 Hz), β (13–30 Hz), and γ (30.5–44 Hz)[53]. The sLORETA algorithm solves the inverse problem—the computation of images of electric neuronal activity based on extracranial measurements—by assuming related orientations and strengths of neighboring neuronal sources that are represented by adjacent voxels. The solution space used in this study and associated lead field matrix are those implemented in the LORETA-Key software. This software implements revisited realistic electrode coordinates[54] and the lead field[55] by applying the boundary element method on the MNI-152 (Montreal Neurological Institute, Canada). The eLORETA-key anatomical template divides and labels the neocortical (including the hippocampus) MNI-152 volume in 6,239 voxels with a size of 5×5×5 mm, based on probabilities returned by the Daemon Atlas (Lancaster et al. 2000). The co-registration makes use of the correct translation from the MNI-152 space into the Talairach and Tournoux space. Anatomical labeling of significant clusters was done using sLORETA's built-in toolbox.

The log-transformed electric current density was averaged across all voxels belonging to the regions of interest (ROIs) for the different frequency bands: δ (2–3.5 Hz), θ (4–7.5 Hz), α (8–12 Hz), β (13–30 Hz), and γ (30.5–44 Hz). The ROIs in the present study are the left and right somatosensory cortex (SSC), the dorsal anterior cingulate cortex (dACC), and pregenual anterior cingulate cortex (pgACC). For the dACC and the pgACC, we do not differentiate between left and right due to their proximity to the midline, as due to volume conduction, laterality is harder to differentiate for areas close to the midline.

3. Lagged phase coherence

Coherence and phase synchronization between time series corresponding to different spatial locations are usually interpreted as indicators of "connectivity." However, any measure of

dependence is highly contaminated with instantaneous, non-physiological contributions due to volume conduction[56]. However, Pascual-Marqui[57] introduced new measures of coherence and phase synchronization taking into account only non-instantaneous (lagged) connectivity, effectively removing the confounding factor of volume conduction. Such "lagged phase coherence" between two sources can be interpreted as the amount of cross-talk or communication between the regions contributing to the source activity[58]. Since the two components oscillate coherently with a phase lag, crosstalk can be interpreted as information sharing by axonal transmission. More precisely, the discrete Fourier transform decomposes the signal in a finite series of cosine and sine waves at the Fourier frequencies [59]. The lag of the cosine waves with respect to their sine counterparts is inversely proportional to their frequency and amounts to a quarter of the period. For example, the period of a sinusoidal wave at 10 Hz is 100 ms; the sine is shifted a quarter of a cycle (25 ms) with the respect to the cosine; then, the lagged phase coherence at 10 Hz indicates coherent oscillations with a 25 ms delay, while at 20 Hz the delay is 12.5 ms, etc.

4. Granger causality

We calculated Granger causality using eLORETA. Granger causality reflects the strength of the information transfer, i.e. effective connectivity (i.e. causal interactions, extract activity of one are of causal influences of one neural element over another) from one region to another by quantifying how much the signal in the seed region is able to predict the signal in the target region[60, 61]. In other words, effective connectivity can be considered as directional functional connectivity. Granger causality is defined as the log-ratio between the error variance of a reduced model, which predicts one time series based only on its own past values, and that of the full model, which in addition includes the past values of another time series. It is important to note that Granger causality does not imply anatomical connectivity between

regions but directional functional connectivity between two sources. In this study, we look at the effective connectivity between the pgACC, dACC, and the left and right SSC.

5. Cross-frequency coupling

Theta-beta, theta-gamma, and alpha-gamma coupling (e.g., by nesting) are proposed to be effective means of communication between cortically distant areas[62]. To verify whether this nesting is present, nesting was calculated for the pgACC, dACC, and the left and right SSC. We computed cross-frequency coupling using eLORETA. Phase–amplitude was chosen over power–power cross-frequency coupling as the former has been shown to reflect a physiological mechanism for effective communication in the human brain[62]. The time-series for each ROI was obtained. Next, these were filtered in the θ (4-7.5 Hz), α (8–12 Hz), β (12.5-30 Hz), and γ (30.5-44 Hz) frequency band-pass regions. The Hilbert transform was then computed on the beta or gamma component and the signal envelope retained. Finally, the Pearson correlation between the theta/alpha component and the envelope of the beta/gamma envelope was computed.

Statistical analysis

For statistical analysis a repeated measures ANOVA for the region of interest, the granger causality, and the cross-frequency analysis with a $p < .05$ significance threshold is used. As the study is characterized by a relatively small sample size (n =15) with a single within-subjects factor, a potential danger is a Type I error. The data are normally distributed as determined by a one-sample Kolmogorov-Smirnov test, and a Mauchly's sphericity test indicated that the variances of the differences between all possible pairs of within-subject conditions are equal. Recent research provided empirical evidence that a repeated measures ANOVA with a correction for the degrees of freedom (i.e., Greenhouse–Geisser correction) can be applied

under the conditions of normality and equal variances. When combined with a single within-subjects factor this controls Type I error rates [63]. Planned comparison tests (i.e., simple contrast analysis) and not a post-hoc analysis was performed, as this method is preferable when specific predefined scientific questions have been determined.

1. Region of interest

We performed a repeated measure ANOVA with the pre- and post-stimulation log-transformed current density for respectively the pgACC, dACC and the left and right SSC as within variables, respectively. These areas and frequency bands were selected based on the a priori hypothesis (see introduction).

Pearson correlations were calculated between the region of interest and the pain score as measured with the VAS for the frequency bands at the left and right SCC, as well as the pgACC. This analysis was corrected for pairwise comparisons using a Bonferroni correction. Pearson correlations were calculated for log-transformed current density of pgACC and PCS.

2. Lagged phase coherence or functional connectivity

The threshold of significance for a given lagged phase coherence value according to asymptotic results can be found as described by Pascual-Marqui [52, 56, 57], where the definition of lagged phase coherence can be found as well. As such, this measure of dependence can be applied to any number of brain areas jointly, i.e., distributed cortical networks, whose activity can be estimated with sLORETA. Measures of linear dependence (coherence) between the multivariate time series are defined. The measures are non-negative and take the value zero only when there is independence and are defined in the frequency domain. Based on this principle lagged linear connectivity was calculated. Time-series of current density were extracted for different regions of interest using sLORETA. Power in all 6,239 voxels was

normalized to a power of 1 and log transformed at each time point. Region-of-interest values thus reflect the log transformed fraction of total power across all voxels, separately for specific frequencies. The regions of interest selected were the pgACC, dACC, and left and right SSC. Lagged phase synchronization/coherence or functional connectivity contrast maps were calculated for the frequency bands: theta (4–7.5 Hz) and alpha (8–12 Hz), based on previous findings. The significance threshold was based on a permutation test with 5000 permutations using threshold t-value at .05. This methodology corrects for multiple testing (i.e., for the collection of tests performed for all voxels, and for all frequency bands).

3. Granger causality

We applied Granger causality analysis to look at the direction of functional connectivity (i.e., effective connectivity). For the theta frequency, we performed a repeated ANOVA including the Granger causality for the effective connectivity pre- and post-stimulation (pgACC→left SSC and left SSC→pgACC; pgACC→right SSC and right SSC→pgACC) as within-subjects variables, respectively.

For the alpha frequency, we performed a repeated including the effective connectivity (pgACC→left SSC, left SSC→pgACC, pgACC→right SSC, right SSC→pgACC, pgACC→dACC, dACC→pgACC) and the pre- and post-stimulation within-subjects variables, respectively. These areas and frequency bands were selected based on the a priori hypothesis (see introduction).

4. Cross-frequency coupling

We performed a repeated measures ANOVA for both the theta-gamma and alpha-gamma phase-amplitude coupling pre- and post-stimulation, and this for both the left and right SSC and

alpha-beta coupling for the dACC as within-subjects variables. Based on the outcome, simple contrast analyses were conducted to look at specific effects.

Results

Effect on Pain

Patients had a score on the VAS of 7.55 (*Sd* = .77) before treatment and 4.85 after treatment (*Sd* = 1.02) showing a significant decrease in pain (F = 161.15, p <.001). For PCS, after stimulation the PCS dropped from 36.33 (*Sd* = 10.17) to 14.60 (*Sd* = 11.49) (F = 9.63, p = .008).

Region of interest analysis

For the pgACC, a significant decrease was revealed for the θ frequency band (F = 14.49, p = .002), but not for α frequency band (F = .61, p = .45)(see figure 1a). Pre-stimulation, a correlation analysis further showed that theta and alpha in the pgACC correlated negatively (r = -.68, p = .005), indicated the higher the log-transformed current density for θ, the lower the log-transformed current density for α, or vice versa. This correlation for the pgACC between the log-transformed current density for θ and α was not obtained post-stimulation (r = -.09, p = .74; see figure 1b). Pre-stimulation, a positive significant correlation was obtained between the VAS pain (pre) and log-transformed current density for θ (r = .65, p = .009), but not for the log-transformed current density for α (r = -.34, p = .22) (see figure 1c). Post-stimulation, no significant correlation was obtained between the VAS pain (post) and log-transformed current density for θ (r = .19, p = .50) or α (r = .07, p = .81) respectively (see figure 1d).

For dACC, for both the α frequency band (F = 9.41, p = .008) and the β frequency band (F = 14.81, p = .002), a decrease in log-transformed current density post-stimulation in comparison to pre-stimulation (see figure 2a) was identified. Pre-stimulation, a positive significant correlation was obtained between the PCS (pre) and log-transformed current density for α (r =

.63, p = .012) and for β (r = .74, p = .002) in the dACC, respectively (see figure 2b). Post-stimulation, no significant correlation was obtained between the PCS (post) and log-transformed current density for α (r = .07, p = .81) or β (r = -.26, p = .34), respectively (see figure 2c).

For the left and right SSC, a significant decrease was revealed for the θ frequency band (left: F = 34.84, p < .001; right: F = 27.68, p < .001) and the γ frequency band (left: F = 38.55, p < .001; right: F = 27.71, p < .001) for post-stimulation in comparison to pre-stimulation (see figure 3a-b). For the left SSC, pre-stimulation a positive significant correlation was found between the VAS pain (pre) and log-transformed current density for the γ frequency band (r = .78, p < .001), but not for the log-transformed current density for θ frequency band (r = -.18, p = .53)(see figure 3c). Post-stimulation, no significant correlation was obtained between the VAS pain (post) and log-transformed current density for θ (r = -.11, p = .70) or γ (r = .39, p = .15), respectively (see figure 3e). For the right SSC, pre-stimulation a positive significant correlation was identified between the VAS pain (pre) and log-transformed current density for γ frequency band (r = .61, p = .015), but not for the log-transformed current density for the θ frequency band (r = -.07, p = .80) (see figure 3d). Post-stimulation, no significant correlation was obtained between the VAS pain (post) and log-transformed current density for θ (r = -.002, p = .99) or γ (r = .48, p = .07) respectively (see figure 3f).

Functional connectivity

Functional connectivity post-treatment for α is increased in comparison to pre-treatment (t = 3.95, p < .05). Increased connectivity was identified between the pgACC and SSC, and the dACC and SSC, as well pgACC and dACC (see figure 4). For θ no significant effect was obtained between pre- and post-stimulation (t = .96, p = .74).

Effective connectivity

For the θ frequency band, a repeated measures ANOVA revealed communication changes between the left SSC and the pgACC (F = 7.58, p = .007) (see figure 5a). For the left SSC→pgACC a significant reduction was shown post-stimulation in comparison to pre-stimulation (F = 6.91, p = .020). An opposite effect was obtained for the communication between pgACC→left SSC showing a significant increase in communication post-stimulation in comparison to pre-stimulation (F = 4.96, p = .043). A similar analysis was applied for communication between right SSC and the pgACC for the θ frequency band, revealing also a significant effect (F = 4.15, p = .040) (see figure 5b). For the right SSC→pgACC a significant reduction was shown post-stimulation in comparison to pre-stimulation (F = 5.85, p = .030). The communication between pgACC→right SSC showing a significant increase in communication post-stimulation in comparison to pre-stimulation (F = 6.16, p = .026). See figure 5c for an overview.

For the α frequency band, a repeated measures ANOVA revealed a significant effect for the communication between left SSC and the pgACC (F = 5.57, p = .018), between right SSC and the pgACC (F = 4.34, p = .036), and between dACC and the pgACC (F = 3.92, p = .043)(see figure 6a-c). For the pgACC→left SSC a significant increase was shown post-stimulation in comparison to pre-stimulation (F = 11.74 p = .004), while no significant effect was demonstrated for left SSC →pgACC (F = 1.08, p = .32) when comparing pre- versus post-stimulation. Also, for the communication from pgACC→right SSC a significant increase was shown post-stimulation in comparison to pre-stimulation (F = 9.35 p = .009), while no significant effect was demonstrated for right SSC →pgACC (F = .55, p = .474). For the communication between dACC and pgACC a significant effect was obtained for pgACC →dACC shown post-stimulation in comparison to pre-stimulation (F = 8.04 p = .013), while

no significant effect was demonstrated for left SSC →pgACC (F = .08, p = .78). See figure 6d for an overview.

Cross-frequency coupling

A significant reduction for θ-γ coupling was obtained for SSC (F = 10.83, p = .002)(see figure 7a). A closer look showed that for both left SSC (F = 11.11, p = .005) and right SSC (F = 6.97, p = .019) a significant decrease in coupling was obtained post-stimulation. Furthermore, a significant reduction in α-β coupling was revealed post-stimulation in comparison to pre-stimulation for dACC (F = 5.94, p = .029) (see figure 7b).

Discussion

This study suggests that chronic pain is indeed an imbalance between the ascending and descending pathways in the brain and that burst spinal cord stimulation reduces this brain imbalance, associated with a reduction in pain and suffering.

This study confirms that chronic pain is associated with increased θ and γ oscillations in the left and right SSC, and that γ oscillations correlate with pain intensity, as previously shown[42]. This is in contrast to a recent systematic review that failed to find gamma changes in chronic neuropathic pain [64]. Furthermore, these findings are also in agreement with the thalamocortical dysrhythmia model[20, 40, 42, 65-70]. The thalamocortical dysrhythmia hypothesis suggests that somatosensory deafferentation leads to a thalamocortical column-specific decrease in information processing, which permits slowing down of resting-state thalamocortical activity from normal α to the θ frequency range[20, 42, 71]. Decreased input also results in a reduction of $GABA_A$-mediated lateral inhibition, inducing γ band activity surrounding the deafferented thalamocortical columns[71]. This γ band activity surrounding θ activity is known as the edge effect[20, 71]. An abnormal increase of θ oscillations in chronic

pain patients has been identified[40, 64, 72]. In addition, the θ-γ coupling that was observed in the SSC, might represent pain-related γ activity[21-23] nested on θ as a carrier wave[73], analogous to what has been proposed for cognitive processing[62].

The dACC, as main hub of the medial 'suffering' pathway, accelerates from θ to α and β frequencies. Both the θ to α and β correlate positively with the suffering component of the pain as measured by the pain catastrophizing scale. The descending pain inhibitory system with the pgACC as main hub, which normally oscillates at rest in θ is reduced in chronic pain[24]. The descending pain inhibitory system accelerates from θ to α suggesting that pain suppression is paradoxically increased, possibly as an attempt, albeit insufficient, to compensate for the increase in pain input[10] as indicated by a negative correlation between the θ and α oscillations[16].

BurstDR spinal cord stimulation induces a significant change in localized brain activity. In both the left and right SSC as well the dACC we identified a significant drop in both θ and γ oscillations for the SSC and in both α and β oscillations for the dACC. This reduction correlates with diminished pain intensity and pain suffering for the SSC and dACC, respectively. This suggests that burst spinal cord stimulation modulates both the lateral and medial pathway. BurstDR stimulation also induces a reduction in θ for the pgACC, but no changes were observed for the α frequency band. However, we do observe a disconnection between the θ and α oscillations post burstDR spinal cord stimulation.

A balance, by definition, requires communication between pain input and suppression between the dACC, SSC, and pgACC. BurstDR stimulation seems to increase communication between brain areas involved in pain processing, as demonstrated by increased functional connectivity between pain input and pain suppression. Indeed, the results of this study indicate increased functional connectivity changes between dACC, SSC, and pgACC for the α band, but not for the θ band. A closer look at the data by analyzing effective connectivity however

indicates that for the θ band, more information is sent from the pgACC to the left and right SSC. This is likely associated with a suppression of the pain and fits with the idea that the imbalance results from reduced pain suppression. For α, increased information is sent from the pgACC to the dACC and both the left and right SSC. These latter findings could suggest that the pgACC is inhibiting activity in both dACC and SSC. This is further confirmed by a reduced θ-γ coupling in the SSC and reduced α-β coupling in dACC. For the SCC areas this is consistent with the thalamocortical dysrhythmia model of pain that proposes that the amount of pathological θ-γ coupling is associated with increasing chronic pain[42] and that a reduction in θ-γ coupling correlates with a decrease in pain due to the γ oscillations that are nested to a lesser extent on the θ [20, 38].

Although chronic pain is one of the most important medical problems facing society, there has been limited progress in finding an objective measure for this fundamentally subjective state. The reason is that a conceptually new way of defining pain from an electrophysiological point of view is still lacking, which could potentially permit an objective quantification of a subjective pain state, purely and entirely based on measuring brain activity. Chronic pain remains difficult to diagnose and manage due to our limited understanding of the underlying mechanisms. Investing in biomarker research has the potential to impact care at multiple stages, including susceptibility screening, diagnosis, prognosis, and more[74]. With accumulating evidence for substantial changes in brain structure and function observed in chronic pain, noninvasive, brain-based measures can likely significantly contribute to the development of pain biomarkers. Because of its scalability, low cost and ease of use in clinical settings, EEG holds great potential as pain biomarker[74]. These new insights of this standard study that define chronic pain as the result of a persisting measurable imbalance between pain input and pain suppression in the brain can help to develop such a biomarker.

Although this study revealed some interesting findings that will help to better understand neuropathic pain, this study has some limitations. First is the low sample size. Research by other groups to cross-validate our findings is warranted. This study was exploratory in nature, aiming to identify potential patterns or relationships in the data. Although our findings confirm the balance model, these findings are a starting point for further investigation. Correction methods for multiple comparisons reduce the probability of making a Type I error but at the cost of decreased statistical power. Because of the unique dataset applying correction methods might result in an overly conservative approach, impeding the identification of potentially important effects. In our cases, a balance between statistical rigor and context-specific considerations is crucial. Furthermore, generalization of the findings of this study require confirmation by other spinal cord stimulation designs such as tonic stimulation, high frequency stimulation, high density stimulation or differential target multiplexed spinal cord stimulation. Research involving pharmacological treatments with NSAIDs, opioids or antiepileptics can also be used to verify the pain imbalance hypothesis.

Traditionally, pain is considered the result of noxious input to the brain via the spinal cord or brainstem, with modification by a descending pain inhibitory pathway in specific situations. This study provides evidence that successful spinal cord stimulation for chronic pain rebalances ascending and descending pain pathways. This means that pain can result from increased noxious input, as in nociceptive pain, with deficient pain suppression, but also from a deficient suppression without increased input, or theoretically even from decreased pain input, if suppression is decreased even more[10]. Furthermore, increased noxious input doesn't necessarily lead to pain, as long as pain suppression equals input.

In summary, this study demonstrates that non-pharmacological treatment using burstDR spinal cord stimulation improves this pain imbalance. This fundamentally new concept of seeing pain as an imbalance disorder in the brain has large implications, not only as a basis for

finding an objective measure for a subjective pain state, but also for developing better pain medication, novel neurostimulation designs, and subtyping pain. Furthermore, in view of the analogy of the underlying pathophysiology of pain, tinnitus, depression, Parkinson's disease[42], and slow wave epilepsy[20], there is no reason to believe this concept could not be extended to these other subjective states.

Conflicts of interest

Dirk De Ridder has IP for burst stimulation. Sven Vanneste has no conflicts of interest to declare.

References

1. Jensen, M.P., M.A. Day, and J. Miro, *Neuromodulatory treatments for chronic pain: efficacy and mechanisms.* Nat Rev Neurol, 2014. **10**(3): p. 167-78.
2. Gaskin, D.J. and P. Richard, *The economic costs of pain in the United States.* J Pain, 2012. **13**(8): p. 715-24.
3. Price, D.D., *Psychological and neural mechanisms of the affective dimension of pain.* Science, 2000. **288**(5472): p. 1769-72.
4. Rainville, P., et al., *Pain affect encoded in human anterior cingulate but not somatosensory cortex.* Science, 1997. **277**(5328): p. 968-71.
5. Kong, J., et al., *Exploring the brain in pain: activations, deactivations and their relation.* Pain, 2010. **148**(2): p. 257-67.
6. Fields, H., *State-dependent opioid control of pain.* Nat Rev Neurosci, 2004. **5**(7): p. 565-75.
7. Eippert, F., et al., *Activation of the opioidergic descending pain control system underlies placebo analgesia.* Neuron, 2009. **63**(4): p. 533-43.
8. De Ridder, D. and S. Vanneste, *Burst and Tonic Spinal Cord Stimulation: Different and Common Brain Mechanisms.* Neuromodulation, 2016. **19**(1): p. 47-59.
9. Bushnell, M.C., M. Ceko, and L.A. Low, *Cognitive and emotional control of pain and its disruption in chronic pain.* Nat Rev Neurosci, 2013. **14**(7): p. 502-11.
10. De Ridder, D., D. Adhia, and S. Vanneste, *The anatomy of pain and suffering in the brain and its clinical implications.* Neurosci Biobehav Rev, 2021. **130**: p. 125-146.
11. De Ridder, D. and S. Vanneste, *The Bayesian brain in imbalance: Medial, lateral and descending pathways in tinnitus and pain: A perspective.* Prog Brain Res, 2021. **262**: p. 309-334.

12. Flor, H., et al., *Phantom-limb pain as a perceptual correlate of cortical reorganization following arm amputation.* Nature, 1995. **375**(6531): p. 482-4.

13. Ossipov, M.H., K. Morimura, and F. Porreca, *Descending pain modulation and chronification of pain.* Curr Opin Support Palliat Care, 2014. **8**(2): p. 143-51.

14. Vanegas, H. and H.G. Schaible, *Descending control of persistent pain: inhibitory or facilitatory?* Brain Res Brain Res Rev, 2004. **46**(3): p. 295-309.

15. Yilmaz, P., et al., *Brain correlates of stress-induced analgesia.* Pain, 2010. **151**(2): p. 522-9.

16. Vanneste, S. and D. De Ridder, *Chronic pain as a brain imbalance between pain input and pain suppression.* Brain Commun, 2021. **3**(1): p. fcab014.

17. De Ridder, D., et al., *Burst spinal cord stimulation for limb and back pain.* World Neurosurg, 2013. **80**(5): p. 642-649 e1.

18. De Ridder, D., et al., *Pain and the Triple Network Model.* Front Neurol, 2022. **13**: p. 757241.

19. Ploner, M., C. Sorg, and J. Gross, *Brain Rhythms of Pain.* Trends Cogn Sci, 2017. **21**(2): p. 100-110.

20. Llinas, R.R., et al., *Thalamocortical dysrhythmia: A neurological and neuropsychiatric syndrome characterized by magnetoencephalography.* Proc Natl Acad Sci U S A, 1999. **96**(26): p. 15222-7.

21. Babiloni, C., et al., *Human brain oscillatory activity phase-locked to painful electrical stimulations: a multi-channel EEG study.* Hum Brain Mapp, 2002. **15**(2): p. 112-23.

22. De Pascalis, V. and I. Cacace, *Pain perception, obstructive imagery and phase-ordered gamma oscillations.* Int J Psychophysiol, 2005. **56**(2): p. 157-69.

23. Gross, J., et al., *Gamma oscillations in human primary somatosensory cortex reflect pain perception.* PLoS Biol, 2007. **5**(5): p. e133.

24. Vanneste, S., O. Alsalman, and D. De Ridder, *Top-down and Bottom-up Regulated Auditory Phantom Perception.* J Neurosci, 2019. **39**(2): p. 364-378.

25. Chakravarthy, K., et al., *Burst Spinal Cord Stimulation: Review of Preclinical Studies and Comments on Clinical Outcomes.* Neuromodulation, 2018. **21**(5): p. 431-439.

26. Chakravarthy, K., et al., *Burst Spinal Cord Stimulation: A Systematic Review and Pooled Analysis of Real-World Evidence and Outcomes Data.* Pain Med, 2019. **20**(Suppl 1): p. S47-S57.

27. Chakravarthy, K.V., et al., *Single arm prospective multicenter case series on the use of burst stimulation to improve pain and motor symptoms in Parkinson's disease.* Bioelectron Med, 2020. **6**: p. 18.

28. Deer, T.R., et al., *Novel Intermittent Dosing Burst Paradigm in Spinal Cord Stimulation.* Neuromodulation, 2021. **24**(3): p. 566-573.

29. Bentley, L.D., et al., *Brain activity modifications following spinal cord stimulation for chronic neuropathic pain: A systematic review.* Eur J Pain, 2016. **20**(4): p. 499-511.

30. Niso, G., et al., *Modulation of the Somatosensory Evoked Potential by Attention and Spinal Cord Stimulation.* Front Neurol, 2021. **12**: p. 694310.

31. Witjes, B., et al., *A Review of Effects of Spinal Cord Stimulation on Spectral Features in Resting-State Electroencephalography.* Neuromodulation, 2023. **26**(1): p. 35-42.

32. Hewitt, D., et al., *Pulse Intensity Effects of Burst and Tonic Spinal Cord Stimulation on Neural Responses to Brushing in Patients With Neuropathic Pain.* Neuromodulation, 2022.

33. Yearwood, T., et al., *Comparison of Neural Activity in Chronic Pain Patients During Tonic and Burst Spinal Cord Stimulation Using Fluorodeoxyglucose Positron Emission Tomography.* Neuromodulation, 2020. **23**(1): p. 56-63.

34. Ahmed, S., et al., *Burst and high frequency stimulation: underlying mechanism of action.* Expert Rev Med Devices, 2018. **15**(1): p. 61-70.

35. De Ridder, D., et al., *Burst spinal cord stimulation: toward paresthesia-free pain suppression.* Neurosurgery, 2010. **66**(5): p. 986-90.

36. Saber, M., et al., *Tonic, Burst, and Burst-Cycle Spinal Cord Stimulation Lead to Differential Brain Activation Patterns as Detected by Functional Magnetic Resonance Imaging.* Neuromodulation, 2022. **25**(1): p. 53-63.

37. Chakravarthy, K., et al., *Mechanism of Action in Burst Spinal Cord Stimulation: Review and Recent Advances.* Pain Med, 2019. **20**(Suppl 1): p. S13-S22.

38. De Ridder, D., et al., *Thalamocortical Dysrhythmia: A Theoretical Update in Tinnitus.* Front Neurol, 2015. **6**: p. 124.

39. De Ridder, D., et al., *Phantom percepts: tinnitus and pain as persisting aversive memory networks.* Proc Natl Acad Sci U S A, 2011. **108**(20): p. 8075-80.

40. Stern, J., D. Jeanmonod, and J. Sarnthein, *Persistent EEG overactivation in the cortical pain matrix of neurogenic pain patients.* Neuroimage, 2006. **31**(2): p. 721-31.

41. Tu, Y., et al., *Distinct thalamocortical network dynamics are associated with the pathophysiology of chronic low back pain.* Nat Commun, 2020. **11**(1): p. 3948.

42. Vanneste, S., J.J. Song, and D. De Ridder, *Thalamocortical dysrhythmia detected by machine learning.* Nat Commun, 2018. **9**(1): p. 1103.

43. De Ridder, D., et al., *All bursts are equal, but some are more equal (to burst firing): burstDR stimulation versus Boston burst stimulation.* Expert Rev Med Devices, 2020. **17**(4): p. 289-295.

44. De Ridder, D. and S. Vanneste, *Confusion About "Burst Stimulation".* Neuromodulation, 2020. **23**(1): p. 140-141.

45. De Ridder, D., et al., *Mimicking the brain: evaluation of St Jude Medical's Prodigy Chronic Pain System with Burst Technology.* Expert Rev Med Devices, 2015. **12**(2): p. 143-50.

46. Osman, A., et al., *Factor structure, reliability, and validity of the Pain Catastrophizing Scale.* J Behav Med, 1997. **20**(6): p. 589-605.

47. Volkow, N.D., et al., *Association between age-related decline in brain dopamine activity and impairment in frontal and cingulate metabolism.* Am J Psychiatry, 2000. **157**(1): p. 75-80.

48. Logan, J.M., et al., *Under-recruitment and nonselective recruitment: dissociable neural mechanisms associated with aging.* Neuron, 2002. **33**(5): p. 827-40.

49. Siepmann, M. and W. Kirch, *Effects of caffeine on topographic quantitative EEG.* Neuropsychobiology, 2002. **45**(3): p. 161-6.

50. Moazami-Goudarzi, M., et al., *Temporo-insular enhancement of EEG low and high frequencies in patients with chronic tinnitus. QEEG study of chronic tinnitus patients.* BMC Neurosci, 2010. **11**: p. 40.

51. Congedo, M., *EureKa! (Version 3.0) [Computer Software]. Knoxville, TN: NovaTech EEG Inc. Freeware available at www.NovaTechEEG.* 2002.

52. Pascual-Marqui, R.D., *Standardized low-resolution brain electromagnetic tomography (sLORETA): technical details.* Methods Find Exp Clin Pharmacol, 2002. **24 Suppl D**: p. 5-12.

53. Song, J.J., S. Vanneste, and D. De Ridder, *Dysfunctional noise cancelling of the rostral anterior cingulate cortex in tinnitus patients.* PLoS One, 2015. **10**(4): p. e0123538.

54. Jurcak, V., D. Tsuzuki, and I. Dan, *10/20, 10/10, and 10/5 systems revisited: their validity as relative head-surface-based positioning systems.* Neuroimage, 2007. **34**(4): p. 1600-11.

55. Fuchs, M., et al., *A standardized boundary element method volume conductor model.* Clin Neurophysiol, 2002. **113**(5): p. 702-12.

56. Pascual-Marqui, R. *Instantaneous and lagged measurements of linear and nonlinear dependence between groups of multivariate time series: frequency decomposition*. 2007.

57. Pascual-Marqui, R. *Discrete, 3D distributed, linear imaging methods of electric neuronal activity. Part 1: exact, zero error localization*. 2007.

58. Congedo, M., et al., *On the "dependence" of "independent" group EEG sources; an EEG study on two large databases.* Brain Topogr, 2010. **23**(2): p. 134-8.

59. Bloomfield, P., *Fourier Analysis of Time Series: An Introduction, 2nd Edition*. 2013, New York: Wiley. 288.

60. Geweke, J., *Measurement of lineair dependence and feedback between multiple time series.* J. Am. Stat. Assoc., 1982. **77**: p. 304.

61. Granger, C.W.J., *Investigating causal relations by econometrics models and crosss-spectral methods.* Econometrica, 1969. **37**: p. 424.

62. Canolty, R.T., et al., *High gamma power is phase-locked to theta oscillations in human neocortex.* Science, 2006. **313**(5793): p. 1626-8.

63. Oberfeld, D. and T. Franke, *Evaluating the robustness of repeated measures analyses: The case of small sample sizes and nonnormal data.* Behavior Research Methods, 2012. **45**: p. 792-812.

64. Mussigmann, T., B. Bardel, and J.P. Lefaucheur, *Resting-state electroencephalography (EEG) biomarkers of chronic neuropathic pain. A systematic review.* Neuroimage, 2022. **258**: p. 119351.

65. Cauda, F., et al., *Low-frequency BOLD fluctuations demonstrate altered thalamocortical connectivity in diabetic neuropathic pain.* BMC Neurosci, 2009. **10**: p. 138.

66. De Ridder, D., et al., *Theta-gamma dysrhythmia and auditory phantom perception.* J Neurosurg, 2011. **114**(4): p. 912-21.

67. Sametsky, E.A., et al., *Enhanced GABAA-Mediated Tonic Inhibition in Auditory Thalamus of Rats with Behavioral Evidence of Tinnitus.* J Neurosci, 2015. **35**(25): p. 9369-80.

68. Sarnthein, J., et al., *Thalamocortical theta coherence in neurological patients at rest and during a working memory task.* Int J Psychophysiol, 2005. **57**(2): p. 87-96.

69. Schulman, J.J., et al., *Imaging of thalamocortical dysrhythmia in neuropsychiatry.* Front Hum Neurosci, 2011. **5**: p. 69.

70. Walton, K.D., M. Dubois, and R.R. Llinas, *Abnormal thalamocortical activity in patients with Complex Regional Pain Syndrome (CRPS) type I.* Pain, 2010. **150**(1): p. 41-51.

71. Llinas, R., et al., *Rhythmic and dysrhythmic thalamocortical dynamics: GABA systems and the edge effect.* Trends Neurosci, 2005. **28**(6): p. 325-33.

72. Sarnthein, J., et al., *Increased EEG power and slowed dominant frequency in patients with neurogenic pain.* Brain, 2006. **129**(Pt 1): p. 55-64.

73. Lisman, J.E. and O. Jensen, *The theta-gamma neural code.* Neuron, 2013. **77**(6): p. 1002-16.

74. Zebhauser, P.T., V.D. Hohn, and M. Ploner, *Resting-state electroencephalography and magnetoencephalography as biomarkers of chronic pain: a systematic review.* Pain, 2022.

Figure legends

Figure 1. (a) A comparison between pre and post burstDR spinal cord stimulation identified a significant difference in current density for the θ frequency band in the pgACC after stimulation. No significant difference was found for the α-band. (b) A correlation was shown between the current density for the θ and α frequency band pre-stimulation, but not post-stimulation. (c) an association was identified for the θ frequency band between the current density in pgACC and the pain intensity as measured by a VAS, pre-stimulation. This association was not found for the α-band. (d) No association was shown for the θ and α frequency band between the current density in pgACC and the pain intensity as measured by a VAS, post-stimulation.

Figure 2. (a) A comparison between pre and post burstDR spinal cord stimulation identified a significant difference for both the α and β frequency band current density in the dACC after stimulation. (b-c) The current density for both the θ and α frequency band for dACC correlates with the PCS pre-stimulation, but not after stimulation.

Figure 3. (a-b) A comparison between pre and post burstDR spinal cord identified a significant difference for both the θ and γ frequency band current density in the left and right SSC after stimulation in comparison to before stimulation. (c-d) Pre-stimulation a significant positive correlation was found between the current density at γ for the left and right SSC and the pain intensity as measured by VAS. For the θ frequency band no significant correlation was found between left and right SSC and the pain intensity. (e-f) post-stimulation, no significant correlation was obtained between current density for θ and γ frequency for left and right SSC and the pain intensity as measured by VAS.

Figure 4. Functional connectivity post-treatment for α in comparison to pre-treatment revealing increased connectivity between the pgAAC and SSC, and the dACC and SSC, as well pgACC and dACC.

Figure 5. (a-b) A comparison between pre and post burstDR spinal cord stimulation for effective connectivity from left SSC→pgACC and pgACC→left SSC, as well as the right SSC→pgACC and pgACC→right SSC for the θ frequency band. This revealed for a significant reduction in effective connectivity for both the left SSC→pgACC and the right SSC→pgACC and increased effective connectivity for the pgACC→left SSC and right SSC→pgACC post-stimulation in comparison to pre-stimulation. (c) A summary figure of the results obtained for the θ frequency band.

Figure 6. (a-c) A comparison between pre and post burstDR spinal cord stimulation for effective connectivity from left SSC→pgACC and pgACC→left SSC, the right SSC→pgACC and pgACC→right SSC as well as the dACC→pgACC and pgACC→dACC for the α frequency band. The analysis identified a significant increase in effective connectivity from pgACC→left SSC, pgACC→right SSC, and the pgACC→dACC post-stimulation in comparison to pre-stimulation. (d) A summary figure of the results obtained for the α frequency band.

Figure 7. (a-b) A significant reduction for θ-γ coupling was identified for the left and right SSC and α-β coupling for dACC post-stimulation in comparison to pre-stimulation.

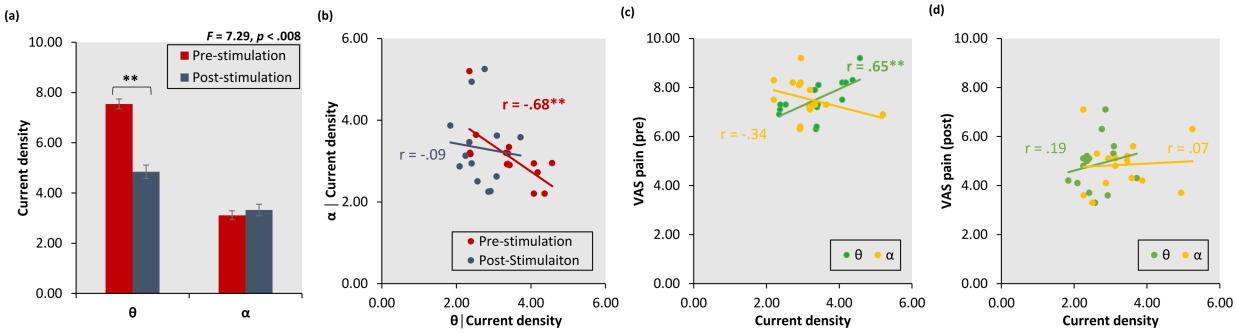

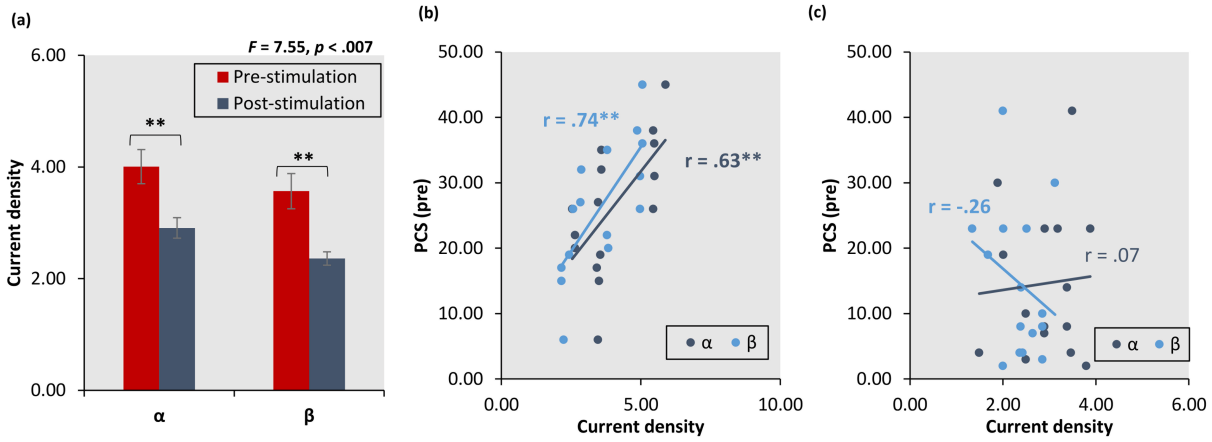

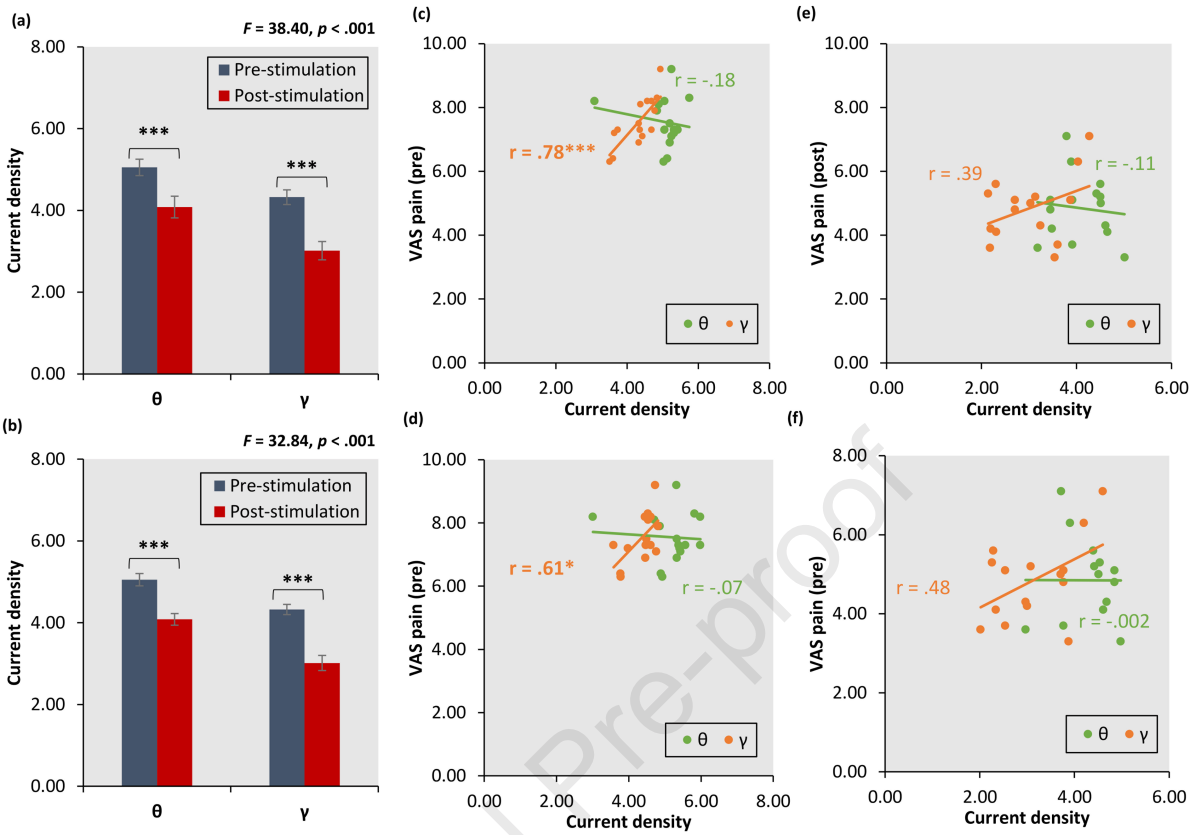

α | post vs pre stimulation (t = 3.95, p < .05)

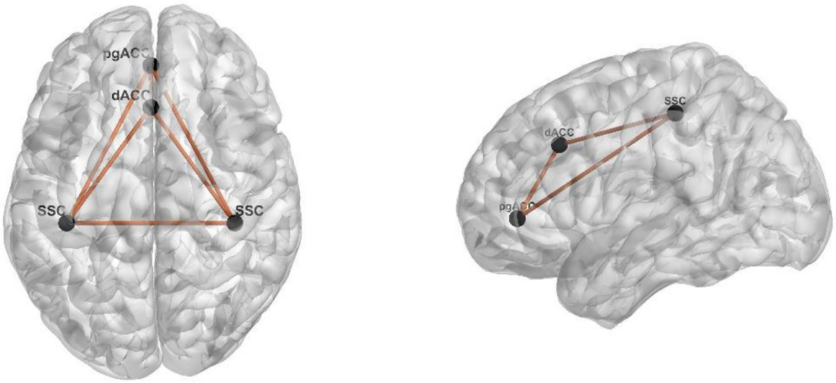

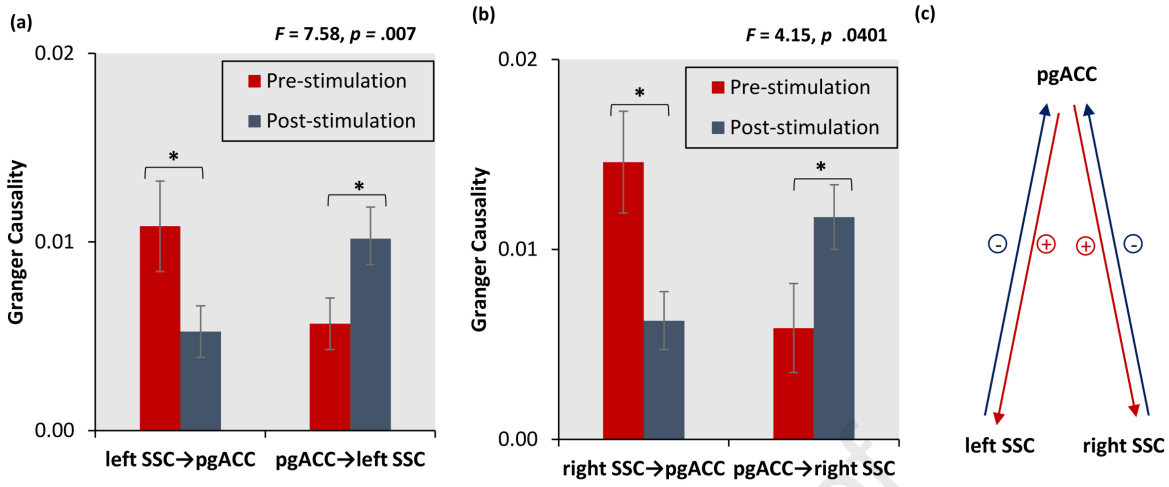

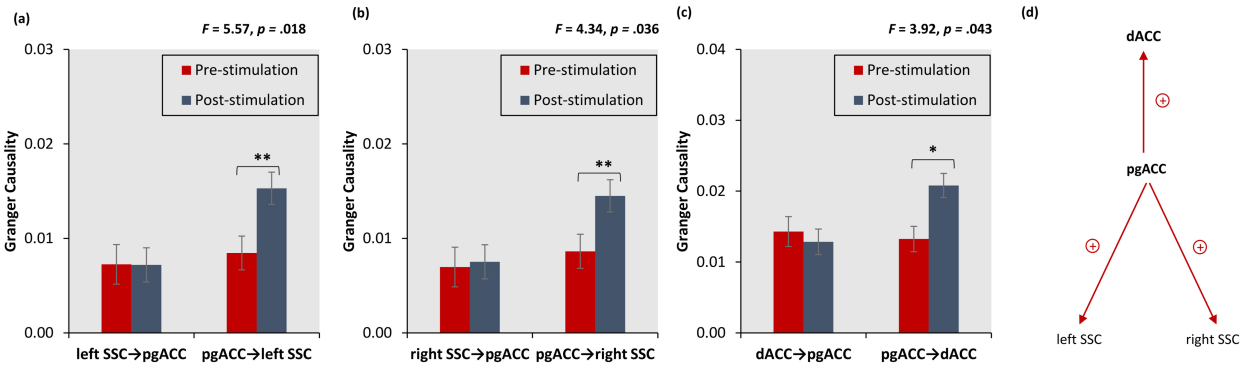

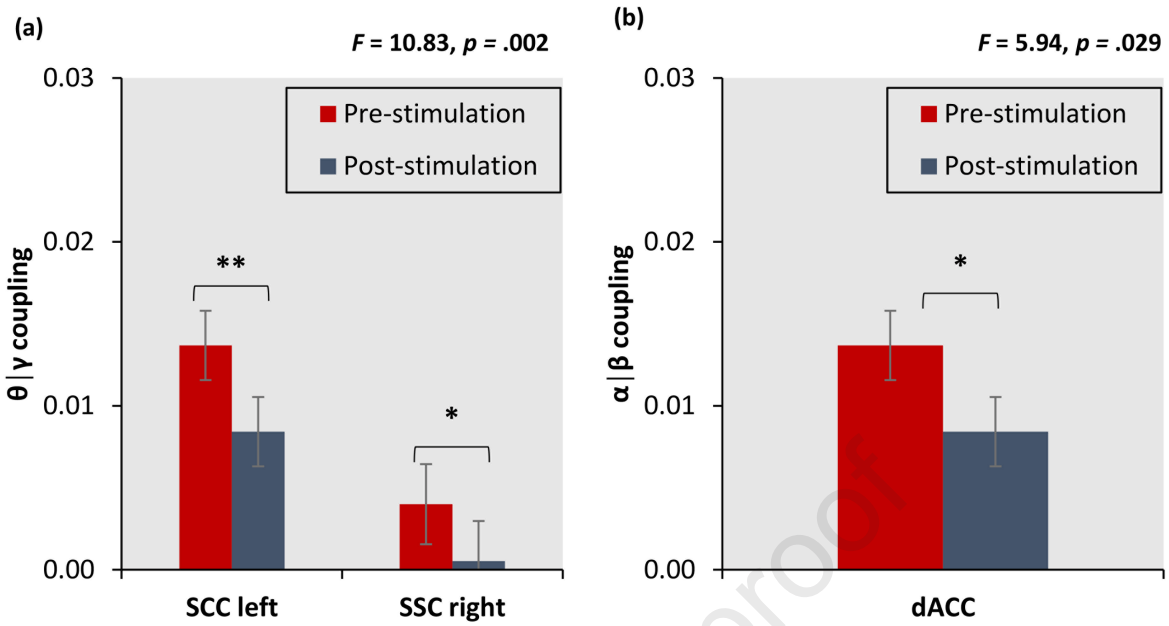

- This study suggests that chronic pain is the result of an imbalance between the ascending and descending pain pathways in the brain.
- BurstDR spinal cord stimulation reduces this imbalance, associated with improvement in painfulness and suffering,
- Electrophysiological measurements including theta-gamma cross-frequency coupling and effective connectivity measures correlate with pain intensity and suffering and are thus potentially usable as objective biomarkers for a subjective pain state.

Conflicts of interest

Dirk De Ridder has a patent for burst stimulation. Sven Vanneste has no conflicts of interest to declare

Author statement

Both authors were involved in study design, data collection, data-analysis and writing up the paper.